Spectroscopic investigation of charge and energy transfer in P3HT/GO nanocomposite for solar cell applications

Fokotsa V. Molefe[1], Mohammed Khenfouch[1,2*], Mokhotjwa S. Dhlamini[1], Bakang M. Mothudi[1]

[1]*Department of Physics, University of South Africa, Private Bag X90, Florida, 1710, South Africa*
[2]*Africa Graphene Center, 2 Boekenhout Street, Florida, Johanesberg, 1709, South Africa*

[*]Corresponding author, E-mail: khenfouch@yahoo.fr

Received: 20 September 2016, Revised: 25 October 2016 and Accepted: 16 December 2016

DOI: 10.5185/amlett.2017.1409
www.vbripress.com/aml

Abstract

As the world demand for energy continue to increase, it is vital to improve renewable energy technologies that will replace conventional fossil fuels. Carbonaceous graphene oxide (GO) is a promising nanomaterial, easy to prepare and scale up to commensurate with industrial requirements. The nanocomposite was prepared in the form of layered structure of GO nanomaterials and poly (3-hexylthiophene) (P3HT) for photovoltaic applications. The X-ray diffraction (XRD) revealed the interaction of P3HT with GO through decrease in lattice spacing. It was evident from scanning electron microscopy (SEM) that the presence of P3HT in GO modified flower like structure to the flaky structures. The interaction of GO with P3HT is presented by various vibrational frequencies in Fourier Transform infrared spectroscopy (FTIR). The increased absorbance and broadening of absorption was observed in the UV-vis spectrum for nanocomposite due to ionic interaction between P3HT and GO. The tunable photoluminescence (PL) measurements showed quenching and shifting of emission spectrum due to charge and energy-transfer. The nanocomposite establish the formation and existence of energy levels upon interaction of GO with P3HT which enhances charge transport. This work provides the direction on coating of thin films for photovoltaic device fabrication.

Keywords: GO, P3HT, nanocomposite, solar cells, charge/energy transfer.

Introduction

More recently, energy scenario has changed leading to substantial increase in energy demand. Renewable energy is a central element in search for energy sustainability. Nano scientists believe nanotechnology could assist in solving many global energy problems faced by the society. The most promising nanomaterial for tackling these challenges is graphene experimentally discovered in 2004 [**1**]. From the year 2010 when Manchester researchers received the Nobel awards on the discovery of graphene validating its importance in research and commercial applications, studies have been conducted to explore carbon nanostructures particularly [**2**]. This is due to outstanding unique properties of graphene that include charge transport, high optical transparency and mechanical flexibility [**3**]. In addition, the remarkable properties of graphene lead to extensive study on its derivatives such as graphene oxide (GO) and reduced graphene oxide (rGO) [**4, 5**]. These nanomaterials are obtainable from graphite which emerged as a precursor for carbon nanostructures, offering the potential of cost effective and large-scale production of graphene based materials [**6**]. Selectively, GO offers a wide range of possibilities to produce graphene based composite materials for various applications in biological imaging [**7**], supercapacitors [**8**] and optoelectronic devices **[3]**.

Currently, numerous routes including microwave [**9**], hydrothermal [**10**] as well as sol-gel process [**11**] and Hummers method [**12**] have been implemented to produce GO nanocomposites. Most of these processes involve a reactive oxygen background which is a vital component for controlling the quality of the thin films. However, Hummer's method is a chemical process that involves pre-intercalation, intercalation, oxidation and reduction chemistry. To date, this top-down approach is the most convenient in terms of high yield and low cost. Moreover, it is environmentally friendly and presents no surface defects while improving dispersion stability of the resulting GO [**13**].

Most importantly when it comes to the efficiency of solar cells is the front panel transparent electrode. Many researchers used metal oxides such as indium tin oxide (ITO) as transparent electrodes due to its low resistance and excellent optical transmission properties in the visible spectrum range [**14**]. However, ITO suffers from brittleness and high production costs hence it cannot be effective for flexible application. Thus, GO is a promising material that possesses acceptable catalytic activity to replace ITO for the construction of flexible electrodes effectively in complex environments. The findings by Koh *et. al.* [**15**] suggested that replacing ITO with

monolayer graphene in organic solar cells yield comparable performance. To create nanocomposite, GO was functionalized using polymeric electron donor (P3HT). Thiophene derivatives from P3HT are well known as high hole mobility materials possessing extensive electron delocalization along the molecular backbone. Hence, P3HT/GO nanocomposite material with higher charge carrier mobility promises to improve device performance [**12**].

GO have been used as a new class of efficient hole and electron extraction materials in solar cells. The creation of nanocomposites using GO as an electron acceptor and P3HT as an electron donor is likely to facilitate charge transport for the emerging area of photovoltaic technology. Sriram *et. al.* [**16**] observed an emission at 407 nm which they attributed to GO interacting with P3HT. The originality of this work lies within the 610 nm emission for P3HT which has not been reported before and the shift to 600 nm emission for P3HT/GO nanocomposite. The new emissions we observed show the creation of new energy levels and the observed emission quenching upon forming P3HT/GO nanocomposite is a preferred property in photovoltaics.

In this study, P3HT/GO nanocomposite was prepared using Hummers method and deposited on a glass substrate. A comparative study on P3HT and P3HT/GO to demonstrate potential applications of bilayer structure is performed. Spectroscopic studies is undertaken to enlighten the functionalization and chemical interactions. The main objective is to investigate the charge transfer properties from a donor (P3HT) to the acceptor (GO).

Experimental

Materials/ chemicals details

Both natural flasks of graphite and P3HT were purchased from sigma Aldrich.

Material synthesis / reactions

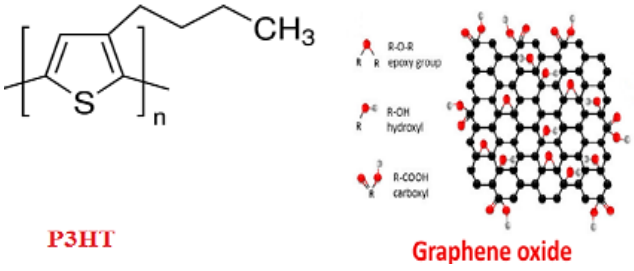

Fig. 1. The idealized chemical structures of used materials.

Fig. 1 presents the chemical structures of the materials used to prepare thin films. The GO sheets were synthesized via modified Hummers method developed by Khenfouch et. al. [**17**]. In order to prevent GO aggregation and restacking, we prepared poly(3-hexylthiophene) P3HT which helps to obtain single or few-layer graphene sheets as follows. The (P3HT) was dispersed in chlorobenzene to prepare solution of 5% concentration. The solution was stirred for 10 minutes on magnetic hot plate maintained at 80℃. Then the temperature was decreased to 50℃ while continuously stirring the solution for 1 hour accompanied by cooling at room temperature. The resulting orange suspension was coated on both a glass slide and GO coated glass slide substrates. The substrates were first cleaned in ultrasonic bath sequentially using deionized water followed by ethanol. Thereafter, substrates were dried at 50℃ prior coating. After coating, the P3HT and P3HT/GO films were dried for 2hrs at 50℃ to remove residual solvents.

Characterizations

The crystalline phases of the nanocomposites were identified by Rigaku Smart Lab diffractometer with CuKα (1.5418Å) radiation. Surface morphologies of the nanocomposites were studied using a scanning electron microscope (SEM) (Shimadzu model ZU SSX-550 Superscan). FTIR spectra were acquired on a PerkinElmer spectrometer in the scan range 400 to 4000 cm^{-1}. The optical measurements were carried out in the 200 to 900 nm wavelength range using a (PerkinElmer Lambda 1050 UV/VIS/NIR Lambda) spectrometer. Luminescence measurements were done using a tunable-photoluminescence (PL) system.

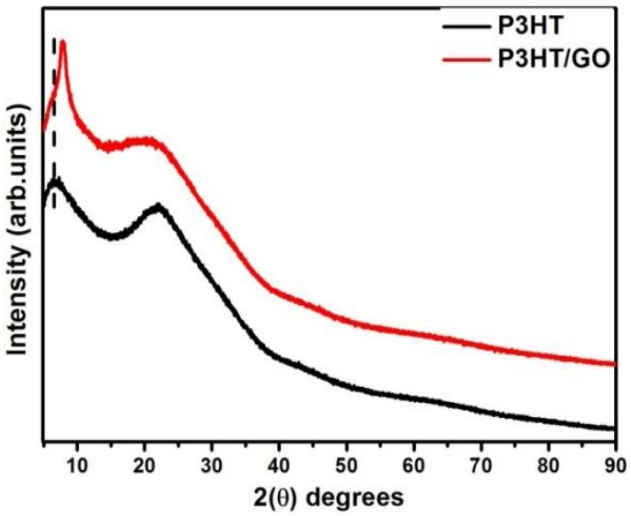

Fig. 2. The XRD patterns of the P3HT and P3HT/GO nanocomposites.

Results and discussion

XRD analysis

Fig. 2 presents the XRD patterns of P3HT and P3HT/GO nanocomposite. For P3HT, the pattern is dominated by an intense thin peak at 2θ=6.65° corresponding to (100) diffraction indicating crystalline phase. In addition to that, a broader peak is observed at 2θ=22.08°. Similarly, the diffraction pattern of the nanocomposite shows the reflections observed in P3HT which proves that the lamellae of P3HT chains adopt an "edge-on" orientation. Stylianakis et. al. [**18**] attributed similar diffraction peaks to the interplanar spacing of the disordered stacking of functionalized GO sheets. The (100) orientation for the nanocomposite reveals a shift to higher diffraction angle mainly due to decrease in lattice spacing. The broad halo observed in the 2θ range 20-40° from both spectrums indicates that the stacked sheets are exfoliated in their

individual nanosheets [**12**]. No other diffraction peaks corresponding to the P3HT crystallites with other orientations such as polymer backbone were observed. Furthermore, GO characteristic peak was observed 2θ=8° which is slightly shifted compared to the normal position which is between 10-11°.

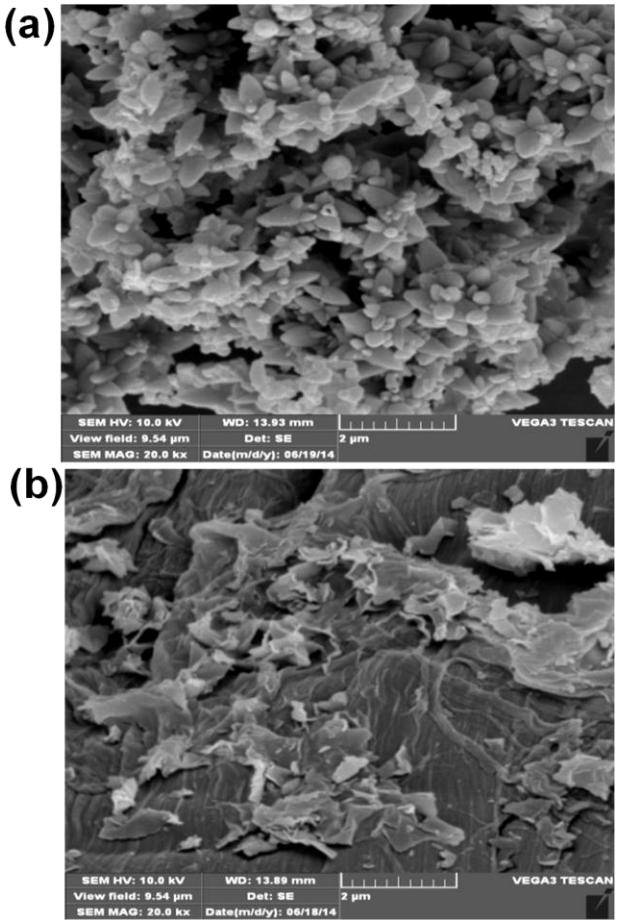

Fig. 3. The SEM images of (a) P3HT and (b) P3HT/GO nanocomposites.

SEM analysis

The surface morphology of prepared P3HT and P3HT/GO nanocomposites were studied through SEM analysis technique and the corresponding images are shown in **Fig. 3**. In **Fig. 3(a)**, P3HT reveals clusters of flower like structures and small oval shapes particles on the surface of the flowers. It should be noted that the surface morphology changed upon deposition of P3HT on top of GO sheets. The SEM image in **Fig. 3(b)** resembles wrinkled and crinkly morphology with flaky like tree leaves structure. The observed flaky structure indicates the dispersion of P3HT on top of GO layers. We suggest that the observed change in surface morphology is due to intimate contact between the basal plane of GO and P3HT. Thus, interaction at this level is most probably between the π-orbitals of the thiophene ring and the π-orbitals of the graphene.

FTIR analysis

The linkage between P3HT and GO in P3HT/GO nanocomposites was analyzed to investigate the bonding interactions using FTIR measurements in transmission mode as shown in **Fig. 4**.

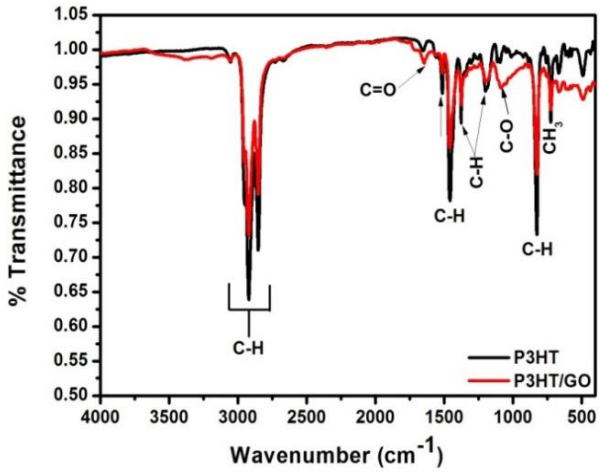

Fig. 4. FTIR spectra of P3HT and P3HT/GO nanocomposites.

The spectra are showing three main characteristic bands of P3HT located at 2960, 2925, and 2855 cm^{-1} which are attributed to aliphatic C-H stretching of P3HT including the 821 cm^{-1} band corresponding to aromatic C-H bending [**19**]. The bending vibration of C-H bond was seen at 1456 cm^{-1}. More vibrational bands emerged at 3372, 3194 and 1081 cm^{-1} characteristic to GO. The C-O bond (1081 cm^{-1}) is attributed to the stretching vibrations which confirms the presence of oxide functional groups after the oxidation process [**20**]. The P3HT/GO spectrum reveals a band at 1648 cm^{-1} which is assigned to the amide carbonyl stretching mode also called Amide I vibrational stretch (ν(C=O)) [**21**]. Thus it is evident from the results that interaction of GO and P3HT leads to the derivatization of both the edge carboxyl and surface hydroxyl functional groups via formation of amides [**20**]. At 721 cm^{-1} we observed a band associated with CH_3 rocking vibration also assigned to methyl rock mode. The observed 1378 cm^{-1} C-H vibration band is suspected to be coming from partial decomposition of the thiophene [**22**]. It is more important to notice that vibrational frequencies observed in P3HT are also available in the P3HT/GO, but their relative intensity decreased after interaction with GO. This significant reduction is presumably caused by oxygenation when P3HT interacts with GO.

UV-vis analysis

Fig. 5 shows the absorbance spectra used to investigate the absorption behavior of P3HT and P3HT/GO nanocomposite. The absorption spectrum of pure P3HT indicates an absorption peak at 490 nm which can be attributed to π-π* transition [**23**]. Compared to the pristine P3HT, the absorption spectrum of P3HT/GO is a bit broader and it shows stronger absorption. The observed broadening and increase in absorption intensity is confirming the contribution of GO in the optical absorption of P3HT/GO layered structure. This can also be due to a decrease in effective conjugation lengths of the chain segments in the amorphous P3HT, localizing the wave function of exciton to a greater extent and therefore increasing its energy [**24**]. The undertaken interaction is

associated with inter-chain order (increase in the disorder of P3HT chains), leading to the enhancement in the absorption spectrum [**25**]. Thus, the enhanced absorption spectrum for P3HT/GO provides the evidence for charge transfer reaction between the donor polymer and the acceptor GO resulting into an optically absorbing nanocomposite.

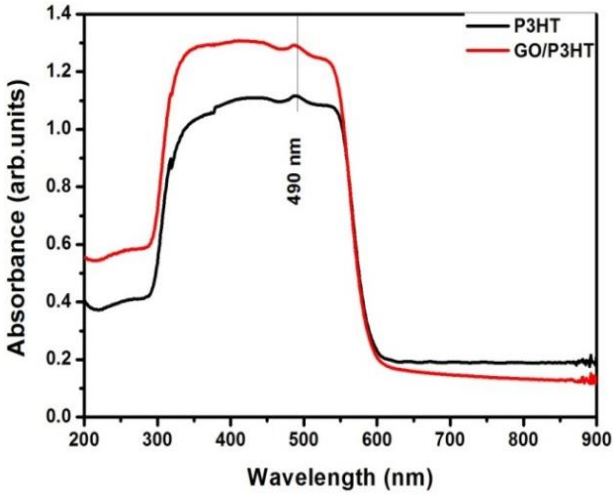

Fig. 5. Absorption spectra of P3HT and P3HT/GO nanocomposites.

Photoluminescence analysis

The excitation dependence of the P3HT and P3HT/GO was taken as shown in **Fig. 6** including contour map which is a matrix of emission spectra acquired at different excitations where the luminescence intensity is a function of excitation and emission wavelength. Upon increasing the excitation wavelength for pure P3HT and P3HT functionalized with GO, we observed gradual emission quenching. This phenomenon illustrates that the excitation wavelength plays similar role on the emission intensity. We presume that the decrease in emission intensity in P3HT and P3HT/GO nanocomposite is due to excitation-based charge transfer. The PL spectrum of pristine P3HT shows a strong fluorescence emission for an excitation wavelength of 360 nm, with a maximum intensity peak at 610 nm. Basically, the emission in P3HT comes from radiative recombination of polaron-exciton pairs into Franck-Condon states [**26**]. It can be clearly seen that the strong PL intensity of P3HT is remarkably reduced after introducing GO indicating that the efficient donor-acceptor charge transfer occurs along the P3HT/GO interface. This is mainly due to enhanced π-π interaction between the backbone of P3HT and GO which affects the planarity of the P3HT because of electrostatic attraction between them [**26**]. Additionally, the quenching is associated to GO flakes acting as the electron acceptor material confining photoemission after strong electron transfer from P3HT to the GO indicating efficient dynamics of exciton dissociation. The changes in intensity may occur due to change in local defects. Zheng *et. al.* [**27**] attributed quenching to the weakening of the interchain interactions of P3HT polymer chains due to the embedding of GO sheets, implying the existence of a large hetero-interface in the P3HT/GO nanocomposite. The observed fluorescence quenching has also been addressed in details by Bkakri *et. al.* [**28**] through energy band diagram of P3HT:Graphene nanocomposite showing possible electrons transfer process at the interface. Thus, this phenomenon illustrates that GO is a promising candidate to act as electron-acceptor for photovoltaic devices. However, Saini *et. al.* [**26**] reported an increase in emission intensity when incorporating GO. Unlike the peak position which was not affected by various excitation wavelengths from 360 to 392 nm, we observed a blue-shift to 600 nm for P3HT/GO nanocomposite. This spectral shift has been attributed to an increase in structural disorder of the P3HT chain [**29**], in correspondence with UV-vis results. From contour map the change in colors from blue to red shows an increase in luminescence intensity. The red region depicts the extent to which the materials were highly luminescent. Importantly, the red region shows shifting in position to lower wavelength for the nanocomposite as compared with pristine P3HT.

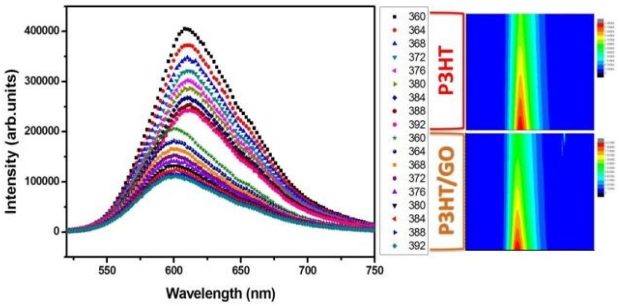

Fig. 6. PL spectra of P3HT and P3HT/GO nanocomposites excited at different wavelengths together with their contour maps.

Table 1 represents the comparison between PL spectra of P3HT and P3HT/GO in the current study and previously reported literature. In the study conducted by Bkakri *et. al* [**27**], emission spectra in the wavelength range 600-750 nm were acquired using an excitation wavelength of 488 nm which lies within the absorption band of P3HT situated between 400 and 600 nm.

Table 1. Comparison between PL emission wavelengths of P3HT and P3HT/GO for the literature **[27]** and current work.

	Literature λ_{EM} **(nm)**	**Current work** λ_{EM} **(nm)**
P3HT	650 and 688	610
P3HT/GO	650 and 688	600

They observed two PL emission maximums at 650 and 688 nm. The noticed emission bands were quenched after addition of graphene. Because of the absence of additional spectral features in the PL spectra of different samples as compared to P3HT, the PL intensity quenching was assigned to electrons transfer from P3HT to graphene. The PL results we are reporting shows emission of P3HT and P3HT/GO in the wavelength range 550-750 nm acquired using various excitation wavelengths that falls within the strong absorption wavelength in **Fig. 5**. The P3HT exhibits PL emission at 610 nm, this emission is quenched for P3HT/GO

nanocomposite. In addition to that, the PL spectra of P3HT/GO nanocomposite show a blue shift to 600 nm. It is well known that the wavelength in PL is associated with the energy positions of triplet state relative to the ground state [**28**]. Thus, the peak position shifts to lower wavelength means that the energy gap between the lowest triplet state and ground singlet state becomes enlarged. So, the shift in the peak position may be related to change in structural irregularity of P3HT, i.e. the structural ordering when depositing P3HT on top of GO reduces the lattice deformation as a result the emission wavelength decreases. This correlates with SEM results where surface morphology for P3HT/GO changed to flaky nanostructures.

Conclusion

As discussed herein, the present study on chemically prepared P3HT/GO layered structure was conducted using various spectroscopic techniques. The interaction of GO with P3HT was shown to affect structural, morphological and optical properties. From FTIR, the presence of oxygen-containing groups validated the serious interaction between GO and P3HT matrix. The enhancement in absorption spectrum provided evidence of donor-acceptor interaction between P3HT and GO. Moreover, the PL results showed that GO confines the photoemission of P3HT resulting in emission quenching. Such interaction between P3HT and GO not only provided superior charge transfer, but also increased energy transfer. In general, the work provides the direction on coating of layered thin film structures for photovoltaics.

Acknowledgements

This work was financially supported by the National Research Foundation (NRF). Further financial support from University of South Africa (UNISA) College of Science Engineering and Technology (CSET) is acknowledged.

Author's contributions

Conceived the plan: MK; Performed the expeirments: FV, MK; Data analysis: FV, MK, MS, BM; Wrote the paper: FV, MK, MS, BM;

References

1. Novoselov, K. S.; Geim, A. K.; Morozov, S. V.; Jiang, D.; Zhang, Y.; Dubonos, S. V.; Grigorieva, I. V.; Firsov, A. A.; *Science*, **2004**, *306*, 666–669. **DOI:** 10.1126/science.1102896
2. Enoki, T.; *Carbon* **2011**, *49*, 2579. **DOI:** 10.1016/j.carbon.2011.01.038
3. Lim, T. Kim, C. S.; Song, M.; Ryu, S. Y.; Ju, S.; *Synth. Met.* **2015**, *205*, 1–5. **DOI:** 10.1016/j.synthmet.2015.03.025
4. Zhu, Y.; Murali, S.; Cai, W.; Li, X.; Suk, J.; Potts, W. J. R.; Ruoff, R. S.; *Adv. Mater.* **2010**, *22*, 3906–3924. **DOI:** 10.1002/adma.201001068
5. Tiwari, A.; (Eds), In the Graphene materials: Fundamentals and emerging applications, John Wiley & Sons, USA, **2015**.
6. Li, B.; Nan, Y.; Zhang, P.; Wang, Z.; Lu, Q.; Song X.; *Diamond Relat. Mater.* **2015**, *55*, 87-94. **DOI:** 10.1016/j.diamond.2015.03.012
7. Misra, S. K.; Pandey, H.; Misra, S. K.; *Int. J. Adv. Pharm.* **2013**, *2*, 1–4. **DOI:** 10.7439/ijap
8. Zang, X.; Li, X.; Zhu, M.; Li, X.; Zhen, Z.; He, Y.; Wang, K.; Wei, J.; Kang, F.; Zhu, H.; *Nanoscale* **201**5, *7*, 7318–7322. **DOI:** 10.1039/C5NR00584A
9. Kim, N.; Xin, G.; Cho, S. M.; Pang, C.; Chae, H.; Curr. *Appl. Phys.* **2015**, *15*, 953–957. **DOI:** 10.1016/j.cap.2015.05.011
10. Zhu, M.; Li, X.; Liu, W.; Cui, Y.; *J. Power Sources* **2014**, *262*, 349–355. **DOI:** 10.1016/j.jpowsour.2014.04.001
11. Hintze,C.; Morita, K.; Riedel, R.; Ionescu, E.; Mera, G.; *J. Eur. Ceram. Soc.* **2016**, *36*, 2923–2930. **DOI:** 10.1016/j.jeurceramsoc.2015.11.033
12. Obreja, A. C.; Cristea, D.; Gavrila, R.; Schiopu, V.; Dinescu, A.; Danila, M.; Comanescu, F. *Appl. Surf. Sci.* **2013**, *276*, 458–467. **DOI:** 10.1016/j.apsusc.2013.03.117
13. Song, J.; Wang, X.; Chang, C. *Journal of Nanomaterials* **2014**, 1–6. **DOI:** 10.1155/2014/276143
14. Farhan, M. S.; Zalnezhad, E.; Bushroa, A. R.; Sarhan, A. A. D.; *Int. J. Precis. Eng. Manuf.* **2013**, *14*, 1465–1469. **DOI:** 10.1007/s12541-013-0197-5
15. Koh,W. S.; Gan, C. H.; Phua, W. K.; Akimov, Y. A.; Bai, P.; IEEE J. Sel. Top. Quantum Electron. **2014**, *20*, 1–8. **DOI:** 10.1109/JSTQE.2013.2247976
16. Sriram, P.; Nutenki, R.; Mandapati, V. R.; Karuppiah, M.; Kattimuttathu, S. I.; *Polym. Compos.* 2015, 1–11. **DOI:** 10.1002/pc.23646
17. Khenfouch, M.; Buttner, U.; Baitoul, M.; Maaza, M.; *Graphene* **2014**, *3*, 7–13. **DOI:** 10.4236/graphene.2014.32002
18. Stylianakis, M. M.; Stratakis, E.; Koudoumas, E.; Kymakis, E.; Anastasiadis, S. H.; *ACS Appl. Mater. Interfaces* **2012**, *4*, 4864–4870. **DOI:** 10.1021/am301204g
19. Yu, D.; Yang, S. Y.; Durstock, M.; Baek, J. B.; Dai, L. M. *ACS Nano*, **2010**, *4*, 5633–5640. **DOI:** 10.1021/nn101671t
20. Ban, F. Y.; Majid, S. R.; Huang, N. M.; Lim , H. N.; *Int. J. Electrochem. Sci.* **2012**, *7*, 4345–4351.
21. Romero-Borja, D.; Maldonado, J.-L.; Barbosa-García, O.; Rodríguez, M.; Pérez-Gutiérrez, E.; Fuentes-Ramírez, R.; de la Rosa, G.; *Synth. Met.* **2015**, *200*, 91–98. **DOI:** 10.1016/j.synthmet.2014.12.029
22. Kovacik, P.; College, O.; "Vacuum Deposition of organic molecules." PhD thesis University of Oxford.
23. Shrotriya, V.; Ouyang, J.; Tseng, R. J.; Li, G.; Yang, Y.; *Chem. Phys. Lett.*, **2005**, *411*, 138–143. **DOI:** 10.1016/j.cplett.2005.06.027
24. Brown, P. J.; Thomas, D.; Köhler, Wilson, A. J.; Kim, J.-S.; Ramsdale, C. Sirringhaus, H.; Friend, R.; *Phys. Rev. B* **2003** *67*, 1–16. **DOI:** 10.1103/PhysRevB.67.064203
25. Arranz-Andrés, J.; Blau, W. J.; *Carbon N. Y.* **2008**, *46*, 2067–2075. **DOI:** 10.1016/j.carbon.2008.08.027
26. Saini, V.; Abdulrazzaq, O.; Bourdo, Dervishi,S. E.; Petre, A.; Bairi, V. G.; Mustafa, T.; Schnackenberg, L.; Viswanathan, T.; Biris, A. S.; *J. Appl. Phys.* **2012**, *112*, 054327. **DOI:** 10.1063/1.4751271
27. Zheng, F.; Xu, W.-L.; Jin, H.-D.; Hao, X.-T.; Ghiggino, K. P; *RSC Adv.*, **2015**, *5*, 89515. **DOI:** 10.1039/c5ra18540h
28. Bkakri, R.; Kusmartseva, O. E.; Kusmartsev, F. V.; Song, M.; A. Bouazizi.; *J. Lumin.* **2015**, *161*, 264–270. **DOI:** 10.1016/j.jlumin.2015.01.014
29. Jung, K. Y.; Bin Park, S.; Anpo, M.; *J. Photochem. Photobiol. A Chem.* **2005**, *170*, 247–252. **DOI:** 10.1016/j.jphotochem.2004.09.003

Supporting information

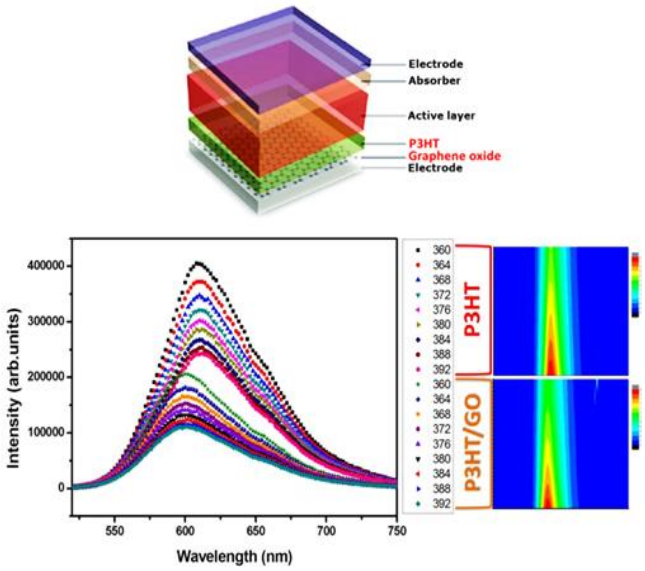

Graphical abstract: P3HT/GO device